Available online at www.sciencedirect.com
ScienceDirect
International Journal of Pharmaceutics 333 (2007) 152–161
INTERNATIONAL JOURNAL OF PHARMACEUTICS
www.elsevier.com/locate/ijpharm

Effect of n-scCO$_2$ on crystalline to amorphous conversion of carbamazepine

Shweta Ugaonkar [a,*], Anthony C. Nunes [b], Thomas E. Needham [a]

[a] *Department of Biomedical and Pharmaceutical Sciences, University of Rhode Island, Kingston, RI 02881, USA*
[b] *Department of Physics, University of Rhode Island, Kingston, RI 02881, USA*

Received 31 May 2006; received in revised form 6 December 2006; accepted 7 December 2006
Available online 14 December 2006

Abstract

A number of studies have been carried out to investigate the crystalline to amorphous conversion of carbamazepine (CBZ) using solid dispersion techniques. In this study we have tried to achieve conversion using a novel technique combining near-supercritical carbon dioxide (n-scCO$_2$) and pharmaceutically acceptable polymers (Na CMC and PVP) of varying molecular weights. Physical mixtures were prepared in two identical sets, one exposed to n-scCO$_2$ treatment and other was untreated. The treated physical mixtures were compared to untreated using PXRD, DSC and USP in vitro dissolution techniques. Routinely used PXRD analysis involves qualitative estimation of the amorphous conversion of a drug. In this work a previously developed mathematical parameter, ratio of ratios (ROR), was utilized to better quantify the crystalline to amorphous conversion of CBZ. The findings from the three methods indicated that only the lowest molecular weight PVP, PVP10k, facilitated significant crystalline to amorphous conversion of CBZ. In vitro dissolution, which is considered as an estimate of bioavailability demonstrated an initial dissolution of CBZ significantly greater in the treated physical mixtures of PVP10k:CBZ than the initial dissolution of the corresponding untreated physical mixtures and pure untreated CBZ.

Keywords: Carbamazepine; n-scCO$_2$; Amorphous; Ratio of ratios (ROR); PVP10k; Initial release

1. Introduction

Carbamazepine (CBZ), an antiepileptic, categorized as Class II as per the Biopharmaceutics classification system (Lőbenberg and Amidon, 2000) occurs in five different polymorphs: triclinic, trigonal, *p*-monoclinic and c-monoclinic forms which are anhydrous and one dihydrate form (Kaneniwa et al., 1987; Krahn and Mielck, 1987; Behme and Brooke, 1990; Kobayashi et al., 2000). CBZ is highly water insoluble (170 mg/l at 25 °C) (Moneghini et al., 2001) and its bioavailability is dissolution rate limited, implying that a small increase in the dissolution rate will result in a multi-fold increase in bioavailability (Nair et al., 2002). The highly crystalline nature of CBZ restricts rapid dissolution. However, a way to overcome this difficulty is to use the amorphous state of the drug thus enhancing dissolution and bioavailability.

Amorphous forms can be induced in a number of different ways, such as milling and compaction of crystals, vapor condensation, supercooling of melts (freeze drying) or precipitation from solution (Hancock and Zografi, 1997). Techniques such as solid dispersion, hot melt extrusion, micronization and formation of solvates, adsorbates or complexes are used in order to enhance the dissolution properties of slightly water insoluble drugs by converting these drugs from the crystalline to amorphous form (Hancock and Zografi, 1997; Moneghini et al., 2001). However these methods often face the problem of physicochemical instability which may arise due to grinding, difficulty in removal of solvents, probable loss of active drug upon evaporation of a liquid organic solvent, as well as from subjecting the drug to high temperatures during the melt extrusion technique.

In this work we have chosen a novel technology using near-supercritical carbon dioxide (n-scCO$_2$) (pressure, 875 psi; temperature, 25 °C) which is below the critical pressure (1070 psi and critical temperature 31 °C; CO$_2$ is in the liquid state) in combination with pharmaceutically acceptable polymers, sodium carboxymethyl cellulose (Na CMC) and polyvinyl pyrrolidone (PVP), of varying molecular weights (MW) in order

* Corresponding author at: Fogarty Hall, 41 Lower College Road, Kingston, Rhode Island 02881, USA. Tel.: +1 401 874 2789; fax: +1 401 874 5787.
E-mail address: shweta@mail.uri.edu (S. Ugaonkar).

0378-5173/$ – see front matter © 2007 Elsevier B.V. All rights reserved.
doi:10.1016/j.ijpharm.2006.12.010

to bring about the crystalline to amorphous conversion of CBZ. It is known that at supercritical conditions, that is, above a substance's critical temperature and pressure, materials behave as gases by exhibiting gaseous properties such as gas like viscosity, thermal conductivity and diffusivity. However, in this state they also exhibit liquid like solvent properties, which may be beneficial in drug solubilization, polymer plasticization and extraction of organic solvents or impurities. Also, the gas like properties significantly enhances mass transfer and promotes extraction (Mukhopadhyay, 2004). In general supercritical fluids are highly tunable solvents which mean small changes in pressure leads to considerable changes in fluid density which in turn leads to changes in the solvent properties (Cansell et al., 2003). In addition $scCO_2$ has low toxicity, is non-flammable and environmentally compatible. It is easily removed from the system once processing is completed as opposed to other methods such as the preparation of solid dispersions where it often is difficult to remove the toxic residual organic solvents. Yet, another advantage of using $scCO_2$ is that it mimics the effect of heat making it important for the processing of thermolabile drug molecules (Kazarian, 2004).

Though supercritical carbon dioxide may seem to have many desirable solvent properties, it is a non-polar solvent having very low polarizability, lesser than that of all hydrocarbons except methane (Dobbs et al., 1986) limiting the solubility of polar solutes. Some other disadvantages include operation at high pressures and high capital investments for equipment.

Amorphous forms being thermodynamically metastable often pose a serious stability threat to the drug products by converting to the more stable crystalline form, thus altering the physicochemical properties of the drug. Often when this change occurs, it cannot be detected by routinely used analytical techniques (Craig et al., 1999). There have been several strategies developed to maintain the amorphous form of drugs for a period of several months and years. One approach is to store the amorphous form of the drug at 40–50 °C below the glass transition (T_g) as proposed by Yoshioka et al. (1995). However, CBZ which has a T_g of approximately 55 °C (Han et al., 2000; Nair et al., 2001), would have to be stored at nearly 0 °C which is not feasible. Hence, an alternative approach for stabilizing amorphous CBZ is to co-solidify it with a polymer having a T_g higher than the drug, thereby increasing the overall T_g of the system (Yoshioka et al., 1995; Hancock et al., 1995). We therefore chose Na CMC and PVP with T_g's of approximately 225 °C, 240 °C, 240 °C, respectively, for LMW, MMW and HMW Na CMC and 180 °C, 160 °C, 175 °C and 185 °C, respectively, for PVP10k, 29k, 55k and 130k to maintain the T_g of the system even after the T_g lowering effects exerted by moisture and CO_2. Also, anticipating interactions between the drug and the polymers a priori such as hydrogen bonding to bring about amorphous conversion was one of the factors in our choice of these polymers. Both have a carbonyl group in their side chains, which has a potential to hydrogen bond with the $–CONH_2$ of CBZ. Lastly, both of the selected polymers find wide applicability in the formulation of solid dosage forms. Hence exploitation of their drug carrier properties using this technique was another criteria of selection. The main objectives of this work were (i) to determine if n-$scCO_2$ aided crystalline to amorphous conversion of pure CBZ or of CBZ when combined with selected polymers; (ii) to study which of the two polymers brought about maximal amorphous conversion and at what ratio; (iii) to examine the effect of reduced particle size of the polymer on the amorphous conversion of CBZ; (iv) to evaluate the effect of processing with n-$scCO_2$ on the dissolution of CBZ or CBZ in combination with several polymer excipients.

2. Materials and methods

2.1. Materials

Crystalline micronized *p*-monoclinic form of CBZ was provided by Hi Tech Pharmacal, NY. For physical mixture preparation of CBZ: 29k and CBZ: 55k mixed in the ratio (9:1), CBZ manufactured by Sigma–Aldrich chemicals was utilized. However, before utilizing CBZ manufactured by Sigma, the identity was confirmed using the X-ray and the DSC scans to be *p*-monoclinic form (same form as provided by Hi Tech Pharmacal). The sodium carboxymethyl cellulose (Na CMC) high molecular weight (HMW) ~700k, medium molecular weight (MMW) ~250k and low molecular weight (LMW) ~90k were donated by Aqualon Ltd. Polyvinyl pyrrolidone (PVP) of MWs 10k, 29k, 55k and 130k were obtained from Sigma–Aldrich chemicals. Methanol (HPLC grade) was supplied by Fischer Scientific. The CO_2 employed in the work was USP grade with 99.8% purity supplied by Medtech gases. All the solvents used were reagent grade.

2.2. Physical mixture preparation

The samples, either the pure drug or mixtures of polymer to drug in ratios of 9:1 (w/w), 1:1 (w/w) and 1:9 (w/w) were prepared in two identical sets. Each set was mixed thoroughly using a magnetic stirrer, then one set was exposed to the high-pressure n-$scCO_2$ assembly (see Fig. 1) for 24 h. Carbon dioxide was allowed to enter slowly, the outlet valve was initially kept open for 2–3 min to displace the internal air. The outlet was then closed and the pressure of the carbon dioxide was allowed to rise slowly, until a pressure of 875–900 psi was reached. This usually occurred in 5 min, which was indicated by the pressure gauges. After the treatment, carbon dioxide was allowed to escape slowly, the sample was removed, secured tightly and

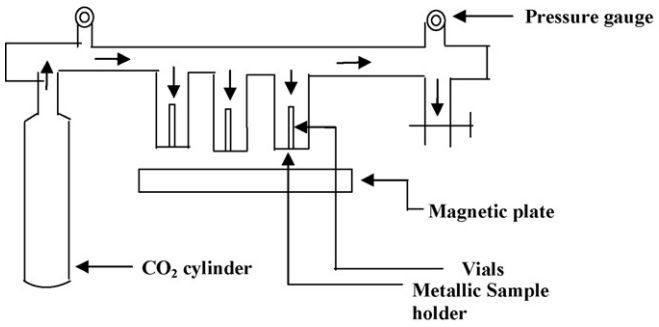

Fig. 1. n-$scCO_2$ treatment apparatus.

stored in a desiccator. The other, control set, was kept untreated. This procedure was carried out at room temperature. All polymers were pre-dried at 80 °C for 16 h and all physical mixtures were kept in a desiccating chamber to minimize the effects of moisture.

2.3. Assay of the total drug content

A standard calibration curve (concentration versus absorbance) of pure CBZ was determined and the fit was found to be linear. Later, known amounts of the prepared samples were dissolved in methanol and the drug content was evaluated spectrophotometrically at 285 nm (Hewlett Packard 8451A diode array spectrophotometer). This wavelength is suitable because CBZ absorbs strongly at this wavelength and the excipients namely Na CMC and PVP do not absorb at or near this wavelength (Nair et al., 2002).

2.4. Particle size measurements

The samples were suspended in the mineral oil and the size was determined microscopically using a ZEISS Axioplan 2 Imaging System.

2.5. Powder X-ray diffraction studies (PXRD)

Samples were characterized using an X-ray diffractometer with Fe Kα radiation, monochromatized by a pyrolitic graphite crystal. The scanning angle ranged from 4° to 76° of 2θ, steps were of 0.06° of 2θ and the counting time was 10 s/step. The current used was 10 mA and the voltage was 35 kV.

Powder X-ray diffraction was chosen to provide a quantitative indicator of the change in the amount of crystalline CBZ in the sample effected by the treatment. An X-ray diffraction pattern (scattered X-ray intensity versus scattering angle "2θ") typically displays two characteristic features. The scattered X-ray intensity arising from crystalline diffraction results in sharp peaks, while that originating in scattering from disordered or "amorphous" material changes slowly with scattering angle. When these two occur in the same sample, the spectrum shows sharp peaks riding on a broad smooth background. These are indicated in Fig. 2. Other sources of background (chiefly scattering from the air and other parts of the instrument) can be made to also vary more slowly with 2θ than the crystalline peaks.

In principle, since the scattered intensity from a given material integrated over all angles depends upon the sample's molecular composition, and is proportional to the amount of material in the X-ray beam and the intensity of that incident beam (Warren, 1969), measuring the fraction of crystallinity of a given sample is possible. The fraction of crystallinity is equal to the total integrated intensity under the sharp Bragg peaks (and above the smooth background on which they sit) to the total integrated intensity of the entire pattern, provided all of the intensity is from the sample in question. In practice, partly because some background arises from sources other than the sample, and partly because of the limited range of the instrument (not all of the entire pattern is accessible), such measurements

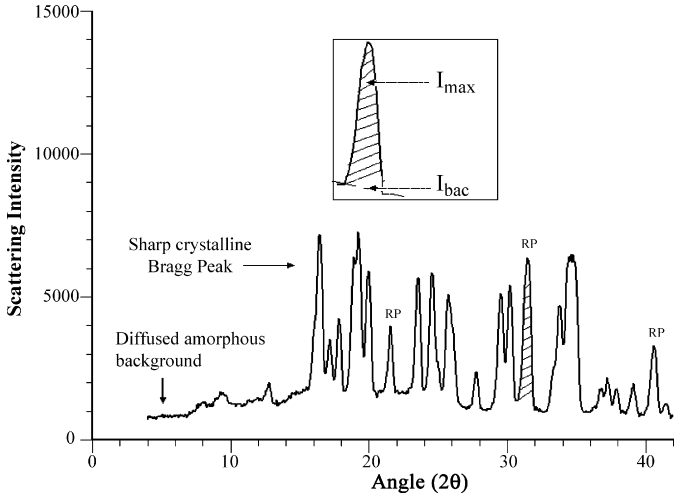

Fig. 2. X-ray diffraction pattern of CBZ showing Bragg peaks and the amorphous background. Inset shows a Bragg peak of area (I_{max}) and intensity background (I_{bac}). RP, representative peaks used for the calculation of ROR.

of absolute crystalline fraction may be difficult to perform. For this reason we have not attempted to measure the absolute crystalline fraction, but rather to monitor the changes of crystalline (Bragg) scattering to amorphous scattering at several regions of the scattering pattern as an indicator of the change crystalline fraction in the sample.

The samples used in this study are composed of CBZ dispersed in a polymer. The highest concentration of drug to polymer used was 1:1 (by weight), and changes of crystalline scattering as indicated by integrated intensity of several Bragg peaks, was small (most of the material remains in its crystalline state in this study). Since most of the scattered background arises from the polymer and instrument, background scattering remains largely unaffected by the small changes in amount of amorphous drug produced by the treatment and so is used as a monitor of the incident X-ray intensity. For a given mixture of drug and polymer, the ratio of the integrated intensity of a Bragg peak I_{max} to the intensity of the background I_{bac} on which it is positioned will depend only upon the amount of crystalline drug present. If some of the drug is converted to an amorphous form (but the chemical composition of the sample remains unchanged), $R = (I_{max}/I_{bac})$ will decrease. We gauge the change in this ratio by measuring it in two parts of one preparation, $R_U = (I_{max}/I_{bac})_U$ one part left untreated while the other is treated with n-scCO$_2$ $R_T = (I_{max}/I_{bac})_T$. With all other parameters held constant, the ratio of these ratios "ROR" (Thumsi, 2004) is a dimensionless number proportional to the fractional change in crystalline content of the sample due to the treatment:

$$\mathrm{ROR} = \frac{R_T}{R_U} \tag{1}$$

We obtain I_{max} and I_{bac} for selected peaks by fitting a narrow region of the scattering pattern $I(2\theta)$ in the neighborhood of the peak to a function composed of a Gaussian and a straight line:

$$I(2\theta) = \frac{I_{max}}{\sigma\sqrt{2\pi}} e^{-(2\theta-2\theta_C)^2/2\sigma^2} + m2\theta + b \tag{2}$$

This function is defined by five parameters. I_{max} is the area under the Gaussian term, $2\theta_C$ is the value of the scattering angle at the peak's center, and σ is the width of the Gaussian. The terms m and b are the slope and intercept of the background line, respectively. This line, along with peak center $2\theta_C$ is used to calculate the value of the background intensity at that point:

$$I_{bac} = m2\theta_C + b \tag{3}$$

These are shown graphically in the inset of Fig. 2. The uncertainty ΔI_{max}, was calculated by the fitting algorithm. The error ΔI_{bac}, was determined from the Poisson counting statistic:

$$\Delta I_{bac} = (\Delta I_{bac})^{1/2}. \tag{4}$$

The error in the ratio of the two numbers is given by (Taylor, 1982):

$$\frac{\Delta R}{R} = \left[\left(\frac{\Delta I_{max}}{I_{max}}\right)^2 + \left(\frac{\Delta I_{bac}}{I_{bac}}\right)^2\right]^{1/2}, \tag{5}$$

and

$$\frac{\Delta ROR}{ROR} = \left[\left(\frac{\Delta R_U}{R_U}\right)^2 + \left(\frac{\Delta R_T}{R_T}\right)^2\right]^{1/2}. \tag{6}$$

To be certain that the drug was evenly dispersed throughout the polymer, and that the grains of both polymer and drug are sufficiently small to not introduce artifacts, the test sample of high MW polymer, PVP130k, was ground and sieved before measuring diffraction patterns.

Samples were mounted as a powder several millimeters thick, held together by a small amount of binder (giving negligible scattering), and pressed onto a steel plate roughly 2 cm × 2 cm in area. This thickness is effectively infinite (X-rays do not penetrate to the bottom of the powder) as indicated by the lack of any iron peaks present in the scattering pattern, so that scattered intensity is not sensitive to variations in sample thickness.

Because these materials are hygroscopic, the instrument's sample stage was placed inside a 10 cm diameter cylindrical desiccator with (1/4) mil plastic windows (producing negligible background scatter). With it, sample weight remained constant, and its appearance and diffraction pattern were stable over the time any sample was left on the instrument.

ROR was measured at three different values of 2θ, indicated by 'RP' in Fig. 2. These were chosen as they are relatively intense and adequately separated from neighboring peaks to permit the above-described analysis. They have been indexed by association with the Form-III carbamazepine crystal structure quoted by (Lang et al., 2002). The lowest angle peak ($2\theta_C = 23.5°$) is the (1, 1, 1) reflection. The middle peak ($2\theta_C = 31.4°$) is an irresolvable quartet made up of the (0, 3, 1), (2, 0, −3), (2, 1, −2) and (0, 2, 3) reflections. The highest angle peak ($2\theta_C = 40.6°$) is also an irresolvable quartet composed of the (2, 2, −4), (0, 4, 0), (1, 2, 3) and the (0, 0, 5) reflections. The fact that these reflections sample widely different directions in reciprocal space, and that the ROR of any one agreed within statistics with the others of any given sample, is evidence that preferred orientation was not a concern. Also, results were statistically reproducible with samples prepared identically but months apart, further supporting this assertion.

This approach is of limited use as it requires that the crystal not change polymorph, but when applicable it is simple to use, and produces robust results.

2.6. Differential scanning calorimeter (DSC)

Differential calorimetric studies were performed using TA instruments DSC Q100. Physical mixtures weighing approximately 2 mg were placed in the aluminum pans and heated at the scanning rate of 10 °C per min from 0 °C to 250 °C. The instrument was calibrated using Indium. The samples were purged using nitrogen at the flow rate of 50 ml/min.

2.7. Determination of drug dissolution

Carbamazepine release profiles were obtained using the USP XXIX, type 2 apparatus, 75 rpm, 900 ml of distilled water as dissolution medium, $T = 37 \pm 0.1$ °C and sink conditions ($C < 0.2C_s$). The sample mixtures (powder form) containing CBZ equivalent to 20 mg was used to study the dissolution profile. Aliquots were withdrawn at 0 min, 5 min, 10 min, 20 min, 30 min, 40 min, 50 min, 60 min, 90 min and filtered using 45 μm PVDF filter. Absorbance was recorded at 285 nm using an UV spectrophotometer. The experiment was carried out in six replicates. The dissolution profiles of the treated samples were compared with that of pure CBZ and the controls under the same conditions.

3. Results and discussion

3.1. X-ray results

The identity of CBZ was compared to the literature using PXRD and found to be the *p*-monoclinic form. Initially a 9:1 (polymer:CBZ) ratio was evaluated because literature studies have demonstrated enhanced dissolution at very high ratios of polymer:drug (Simonelli et al., 1976; Kearney et al., 1994).

From Fig. 3a and b which compares untreated and treated XRD scans of the pure CBZ, it is apparent that n-scCO_2 treatment did not elicit the appearance of new, or the disappearance or reduction in the intensities of existing peaks. This indicated that n-scCO_2 did not promote amorphous or polymorphic conversion of CBZ. A similar observation was noted when XRD scans of Na CMC (LMW):CBZ at a 9:1 ratio with and without treatment were analyzed (Fig. 3c and d). However, a significant reduction in the intensity of the peaks was seen in the scans of the treated (PVP10k:CBZ) mixture (Fig. 3f) compared to the XRDs of the corresponding untreated mixtures (Fig. 3e). This was attributed to the partial amorphous conversion of CBZ. However, visual qualitative estimation of XRD scans can sometimes be misleading as the effects may be subtle. In order to quantify the reduction in the peak intensity, ROR which is explained above was utilized to evaluate crystalline to amorphous conversion (Thumsi, 2004).

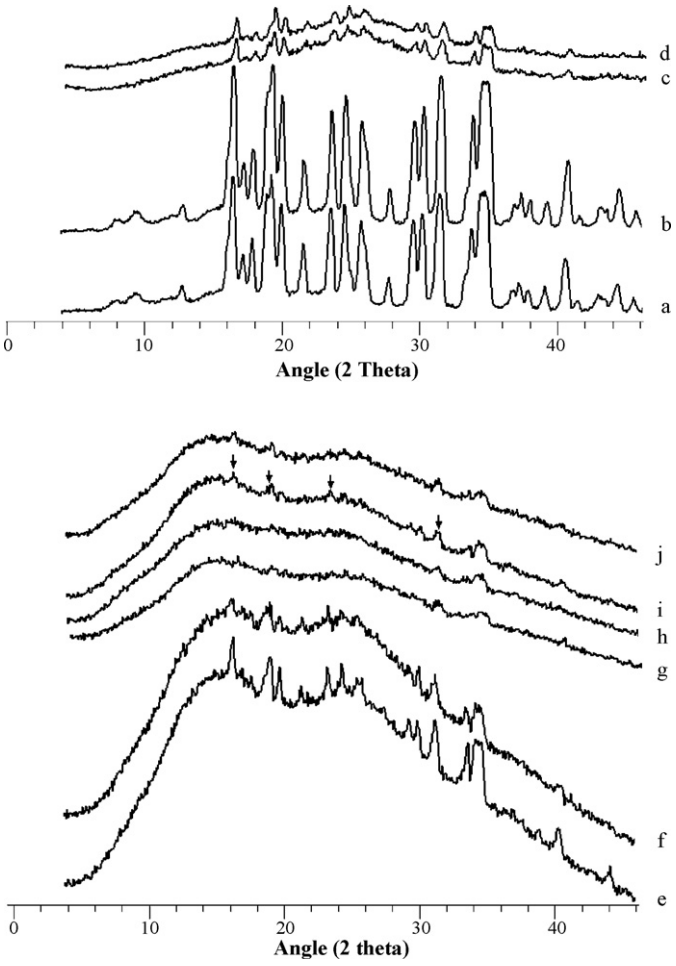

Fig. 3. PXRD scans of untreated and treated physical mixtures of polymers and CBZ at different ratios. (a) CBZ-untreated, (b) CBZ-treated, (c) Na CMC (LMW):CBZ (9:1)-untreated, (d) Na CMC (LMW):CBZ (9:1)-treated, (e) PVP10k:CBZ (9:1)-untreated, (f) PVP10k:CBZ (9:1)-treated, (g) PVP130k (unground, unsieved):CBZ (9:1)-untreated, (h) PVP130k (unground, unsieved):CBZ (9:1)-treated, (i) PVP130k (ground, sieved):CBZ (9:1)-untreated, and (j) PVP130k (ground, sieved):CBZ (9:1)-treated.

If CBZ in combination with a polymer were to be completely converted to the amorphous form then, the crystalline structure of CBZ would become disordered leading to the disappearance of the Bragg peaks. The scattering from the disordered CBZ would be dispersed over a broad range of angles adding to the polymer background intensity (Fig. 4). To quantify the change in peak intensity, and thus evaluate crystalline to amorphous conversion, the ROR was used as described in Section 2.5

When the equations for ROR were applied to the three peaks generated from the PXRD scans for the untreated and treated CBZ, The ROR $\pm$ ΔROR was calculated to be 1.083 ± 0.132. The ROR calculated for the Na CMC (LMW):CBZ samples at a 9:1 ratio was 0.99 ± 0.33. This indicated no significant difference between untreated and treated samples or no conversion from the crystalline to amorphous form. However, ROR $\pm$ ΔROR of 0.39 ± 0.03 for PVP10k:CBZ at a (9:1) ratio indicated amorphous conversion as this value is considerably less than 1, supporting the visual observation.

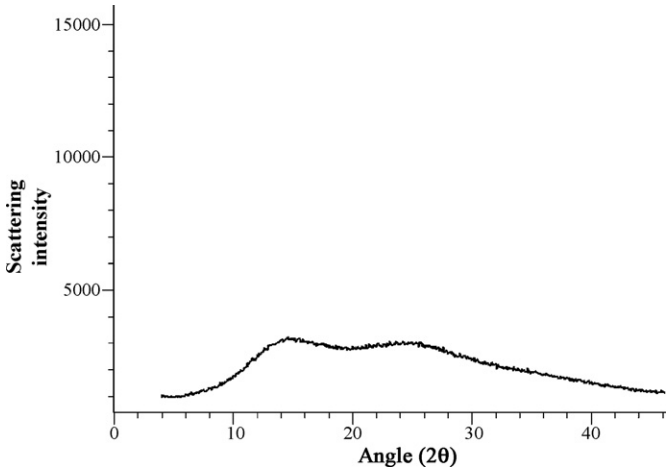

Fig. 4. X-ray scan of polymer background showing absence of crystalline Bragg peaks.

While working with these mixtures it was found that the Bragg peaks in the PVP130k:CBZ (9:1) mixtures were not distinct and could not be quantified in the untreated as well as the treated samples (Fig. 3g and h). This result can be contrasted with the PVP10k–CBZ mixture where the Bragg peaks underwent reduction in the intensity only upon subjection to the n-scCO_2 treatment. We tried to investigate the reasons for this anomalous behavior.

3.1.1. Effect of particle size

It was determined that there was a considerable difference in particle size between the CBZ particles with an average size of 12 μm and the PVP130k particles with an average size of 1 mm (Fig. 5a and b). Owing to this large particle size difference and knowing that the X-ray beam is only few mm wide, it is hypothesized that the X-ray beam captured the scattering predominantly due to the polymer, disregarding the signal produced by the CBZ crystallite.

By grinding and sieving PVP130k, we reduced the average particle size to 268 μm (Fig. 5c) with the expectation that a more uniform particle size for both components in the mix would eliminate the bias introduced by the X-ray beam intensity. After mixing the ground and the sieved polymer with CBZ at a 9:1 ratio, the crystalline peaks in the mixture became more apparent as indicated by (↓) in Fig. 3i. Analysis to estimate the amorphous change in the treated and the untreated sample mixtures provided no indication of conversion to the amorphous form (refer Fig. 3i and j) as the resulting ROR was 0.97 ± 0.66

In order to evaluate if differences in the molecular weight of a polymer would act as one of the factors that affects the conversion to the amorphous form for CBZ, we tested the Na CMC and PVP of varying molecular weights. The observed ROR $\pm$ ΔROR for the different polymers (all MW):CBZ at a (9:1) ratio are depicted in Table 1. From the table it is obvious that only PVP10k:CBZ mixture showed an appreciable amorphous conversion as the ROR $\pm$ ΔROR was 0.39 ± 0.03, significantly less than 1. For the tested polymers at different MWs we also observed that at a 9:1 ratio of polymer:CBZ, the signal produced was very weak. This was attributed to the minimal quantity of

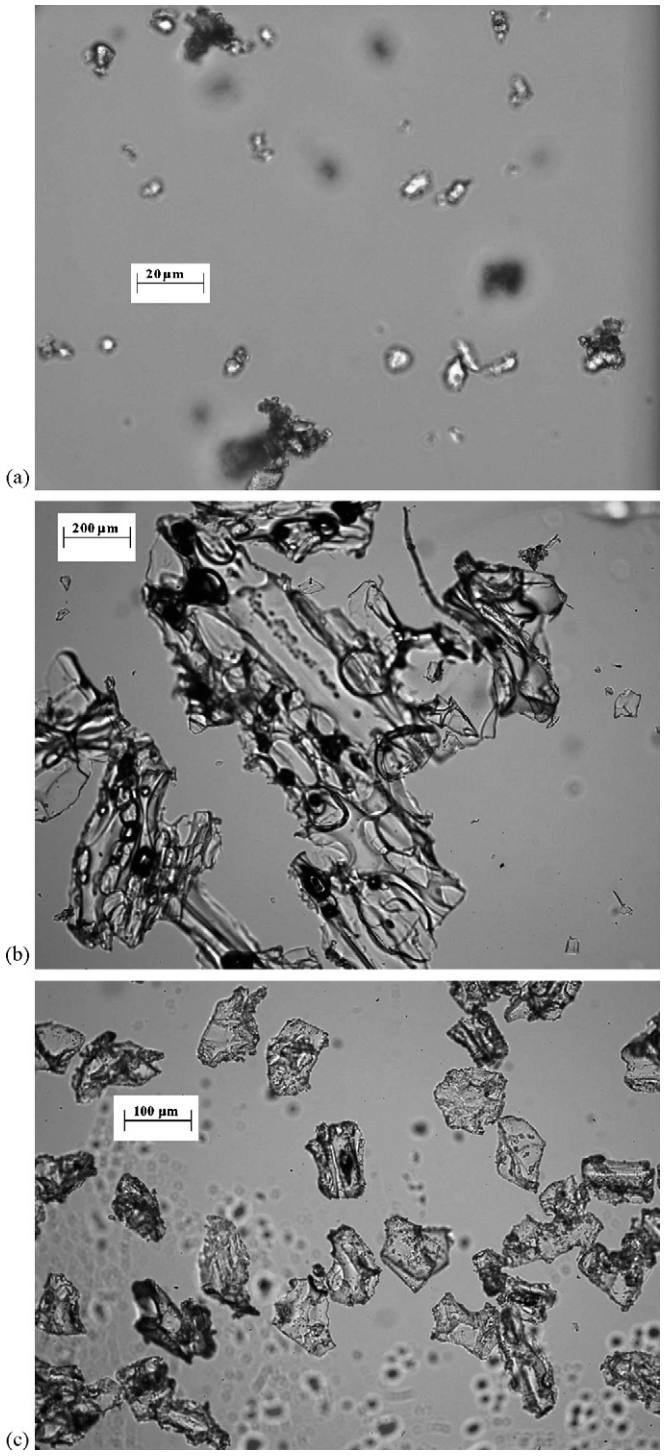

Fig. 5. Microscopic view of CBZ crystallites, unground and ground PVP130k. (a) CBZ crystals (average particle size: 12 μm), (b) unground, unsieved PVP130k (average particle size: 1 mm) and (c) ground, sieved PVP130k (average particle size: 268 μm).

crystalline CBZ as compared to the amount of polymer present. Hence in order to improve the signal to noise ratio, we tested 1:1 and 1:9 ratios of polymer:CBZ. It was postulated that the ratios that contained higher amounts of crystalline CBZ would improve the measurability of the peaks and allow us to obtain more meaningful data. As seen from the results in Table 2, only

Table 1
ROR and ΔROR values for mixtures containing polymer and the drug at a (9:1) ratio

Sample	ROR	ΔROR
Plain CBZ	1.08	0.13
Na CMC (LMW):CBZ	0.99	0.35
Na CMC (MMW):CBZ	0.82[a]	0.32
Na CMC (HMW):CBZ	1.18	0.25
PVP10k:CBZ	0.39	0.03
PVP29k:CBZ	0.85[a]	0.13
PVP55k:CBZ	1.14	0.50
PVP130k(ug, us):CBZ	ND	ND
PVP130k(g, s):CBZ	0.97	0.66

ND, not detectable; ug, unground; us, unsieved; g, ground; s, sieved.
[a] Values not significantly different than 1.

the PVP10k:CBZ mixtures exhibited a ROR, which was statistically less than 1. The RORs for PVP10k:CBZ mixtures were 0.83 and 0.86 at (1:1) and (1:9) ratios, respectively, implying that the mixtures underwent partial conversion to the amorphous form after the treatment. Though some mixtures in Table 2 exhibits a ROR of 0.92 and 0.98, these values are statistically not different from 1.

Hence, from the results obtained in the X-ray studies it was evident that only PVP10k seemed to bring about a significant crystalline to amorphous conversion of CBZ at all the ratios tested.

3.2. DSC results

Nair et al. (2002) have attributed the absence of a drug melting endotherm to the conversion of the drug to its amorphous form. The DSC scans of untreated and treated (LMW) Na CMC and CBZ at 9:1 are shown in Fig. 6a and b, respectively.

The melting endotherms seen in Fig. 6a at 179 °C and at 192 °C are characteristic of the monoclinic form of CBZ. When comparing Fig. 6a and b, it can be seen that both untreated and treated CBZ show both of these melting endotherms. Thus it can be said that no amorphous conversion of CBZ is seen in LMW Na CMC matrix. This observation was also true for MMW and HMW Na CMC.

However, the melting endotherms were absent for all molecular weights of the PVP:CBZ mixtures at 9:1 ratio when they

Table 2
ROR and ΔROR values for mixtures containing PVP10k:CBZ at (1:1) and (1:9) ratios

Ratio	Sample	ROR	ΔROR
1:1	CBZ:PVP10k	0.83	0.05
1:1	CBZ:PVP29k	1.16	0.07
1:1	CBZ:PVP55k	1.03	0.06
1:1	CBZ:PVP130k	0.92	0.05
1:9	PVP10k:CBZ	0.86	0.05
1:9	PVP29k:CBZ	1.02	0.05
1:9	PVP55k:CBZ	0.98	0.05
1:9	PVP130k:CBZ	1.70	0.08

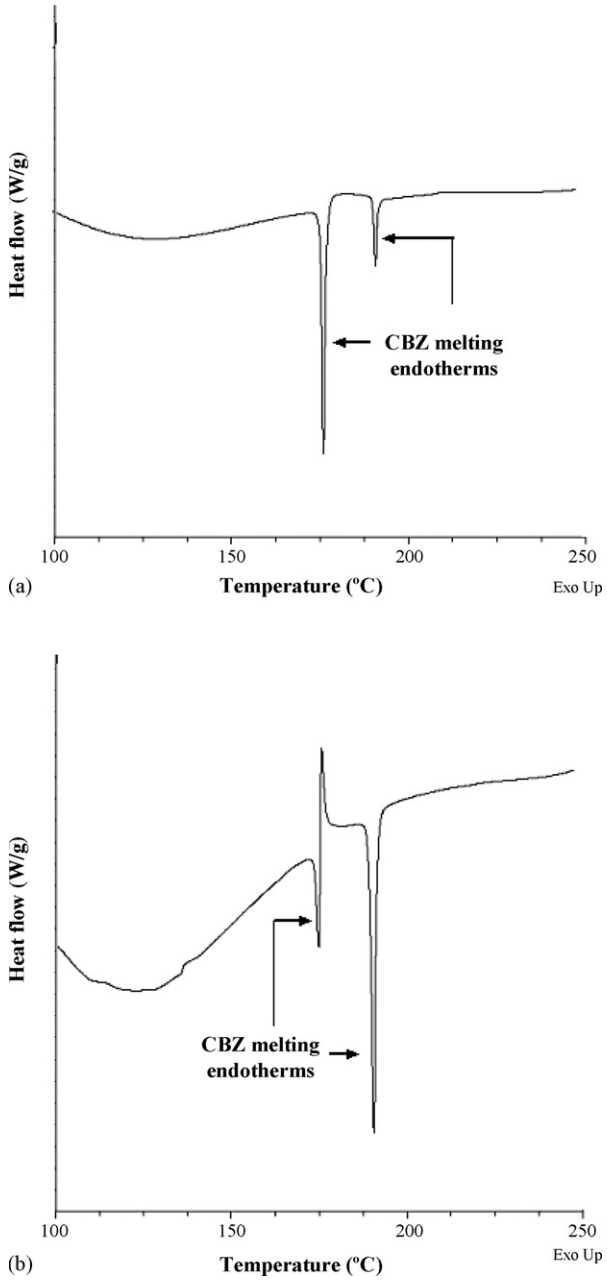

Fig. 6. DSC scans of LMW Na CMC and CBZ. (a) LMW Na CMC:CBZ (9:1)-untreated and (b) LMW Na CMC:CBZ (9:1)-treated.

were subjected to n-scCO$_2$ treatment which suggests crystalline to amorphous conversion of CBZ in these mixtures. At higher drug concentrations such as 1:1, an attenuated drug melting endotherm was observed in the scans of the treated (PVP10k:CBZ) mixture only (see Fig. 7a and b). The scans of other higher MW PVP mixed with CBZ at the same ratio showed no difference in the intensities of the CBZ melting endotherms in the untreated and treated samples, implying no conversion. At a 1:9 ratio for all molecular weights of PVP, there was no difference in the intensities in the melting endotherms of the untreated and treated samples because at this ratio, the mixture was essentially dominated by CBZ (refer Fig. 7c and d). Since the Na CMC matrix was not conducive for amorphous conversion of CBZ as proven by the X-ray and the DSC studies, we decided to eliminate it from further investigation.

3.3. Dissolution studies

The dissolution profiles for the pure drug, untreated and treated PVP10k:CBZ mixtures at a 9:1 ratio are shown in Fig. 8. We observed that when the dissolution profile of the pure drug was compared to those for drug–polymer mixtures, there was an initial increase in the rate of release for all the PVP–CBZ mixtures in the initial 30 min. However the amount of the drug that dissolved reached a plateau and was essentially the same for all samples after approximately 1 h. It was difficult to predict after visual examination if the n-scCO$_2$ treatment had a significant effect on the rate of release of CBZ when compared to the rate of release for the untreated mixtures. In order to evaluate the difference in release for the compared systems quantitatively and to determine if the profiles were significantly different, we fitted the dissolution data to an inverse exponential curve and compared the percent release at '0' minutes for all the systems. The curve as seen in Fig. 9 is represented by the equation:

$$Y = A(1 - e^{-x/\tau}) + B \quad (8)$$

where Y is the % drug released, A the difference between the total release and the release at the intercept, x the time (min), τ a time constant which represents the time required for drug release from the entire system (min^{-1}), and B is the intercept representing the % release of the drug at '0' minutes.

The root mean square error (RMSE) of the fit was comparable in each case. The error calculated for the dissolution at each time point indicated that this equation provides an appropriate description of the time dependent dissolution curves. We extrapolated the curve to '0' minutes and found the intercept value (B). The percent release at '0' minutes indicates a very rapid dissolution presumably resulting from the amorphous fraction of the drug. The values for the parameters fitted to the dissolution curve as discussed in Eq. (8) are illustrated in Fig. 9 for the treated (PVP10k:CBZ) mixture at a 9:1 ratio. As seen in Table 3,

Table 3
Estimated amount of CBZ dissolved at $t = 0$ for PVP–CBZ mixtures at (9:1), (1:1) and (1:9) ratios

Ratio	Sample	% Release at '0' min (intercept values)-treated
–	Pure CBZ	1.25 ± 3.12
9:1	PVP10k:CBZ	21.0 ± 1.12
9:1	PVP29k:CBZ	7.93 ± 0.8
9:1	PVP55k:CBZ	9.47 ± 2.32
9:1	PVP130k:CBZ	15.8 ± 0.823
1:1	PVP10k:CBZ	14.20 ± 0.848
1:1	PVP29k:CBZ	8.43 ± 0.878
1:1	PVP55k:CBZ	5.14 ± 1.38
1:1	PVP130k:CBZ	6.39 ± 1.03
1:9	PVP10k:CBZ	4.94 ± 1.72
1:9	PVP29k:CBZ	2.22 ± 1.60
1:9	PVP55k:CBZ	5.43 ± 3.13
1:9	PVP130k:CBZ	3.38 ± 0.82

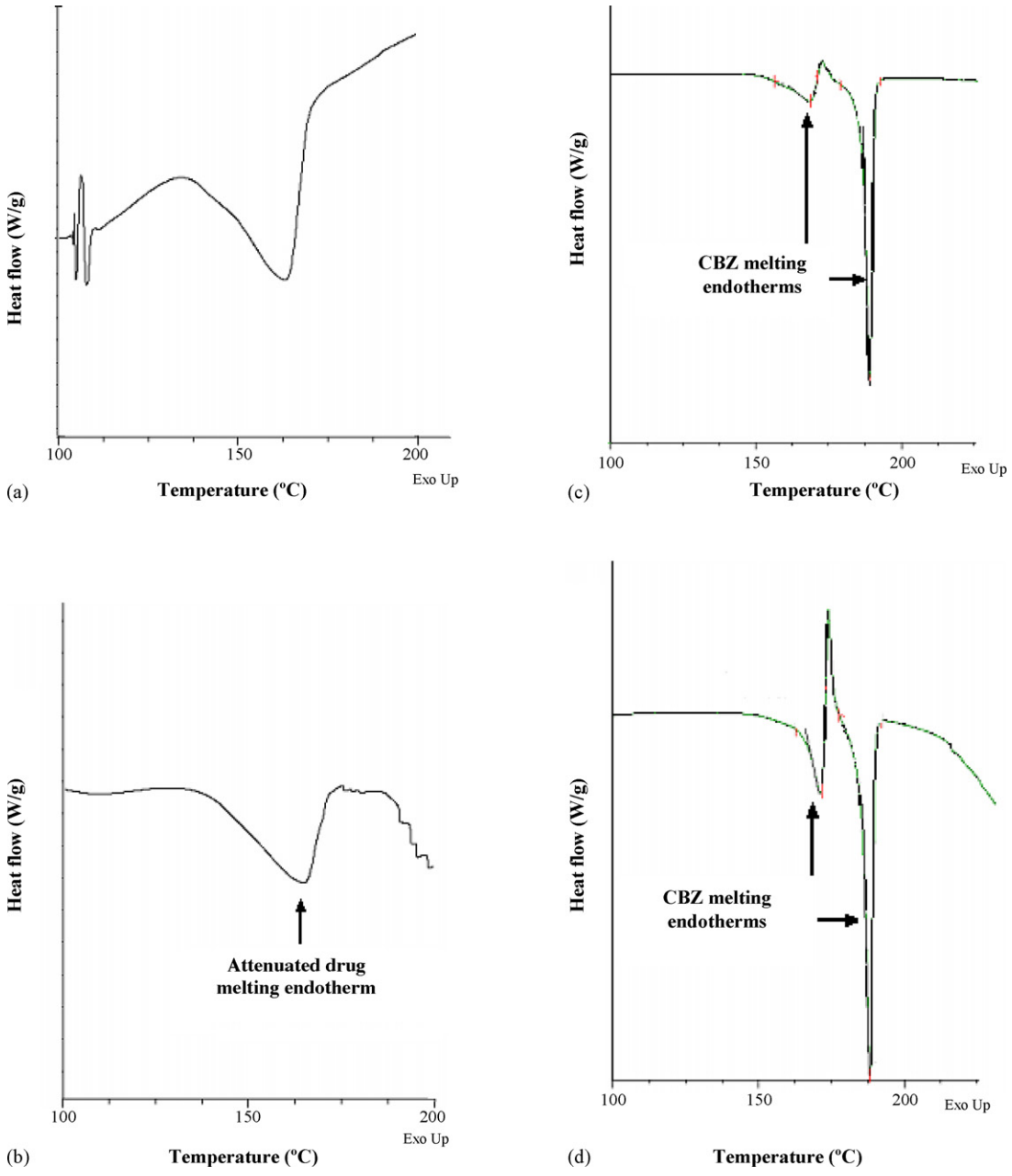

Fig. 7. DSC scans of PVP10k and CBZ at different ratios. (a) PVP10k:CBZ (1:1)-untreated, (b) PVP10k:CBZ (1:1)-treated, (c) PVP10k:CBZ (1:9)-untreated and (d) PVP10k:CBZ (1:9)-treated.

at the 9:1 ratio for the various molecular weights of PVP:CBZ mixtures that were tested, the PVP10k:CBZ when treated with n-scCO_2 showed the highest release of 21.0% at time equal to zero. This is compared to a zero time release of 7.93%, 9.47% and 15.8% for mixtures of the other high MW PVP polymers at the 9:1 ratio mixtures. Similarly at the 1:1 ratio of PVP:CBZ, the treated PVP10k:CBZ mixture showed the highest percent release of 14.2 as compared to 8.43, 5.14 and 6.39 for the other treated mixtures of high MW PVPs.

It should be noted that as the amount of CBZ in the ratio increases, the dissolution process increasingly becomes more drug controlled as opposed to being polymer controlled when higher polymer content was present in the mixtures (Craig, 2002). Thus, due to the high content of drug at the 1:9 ratio for all molecular weights of PVP:CBZ, the percent drug released (4.94, 2.22, 5.43 and 3.38) at $t = 0$ min, is not significantly different than the amount of pure CBZ released at $t = 0$. Doshi et al. (1997) and Moneghini et al. (2001) also reported a direct correlation between the increase in polymer content and dissolution enhancement for CBZ and polyethylene glycol mixtures. Both the X-ray and the DSC studies carried out in this work are in agreement with this observation. The value of ROR increased (implying lesser amorphous conversion) as the amount of CBZ in the mixture increased. The ROR of 0.39 ± 0.03 for the 9:1 ratio of PVP10k:CBZ increased to 0.83 ± 0.05 at a 1:1 ratio, and further increased to 0.86 ± 0.05 at a 1:9 ratio of PVP10k:CBZ. A

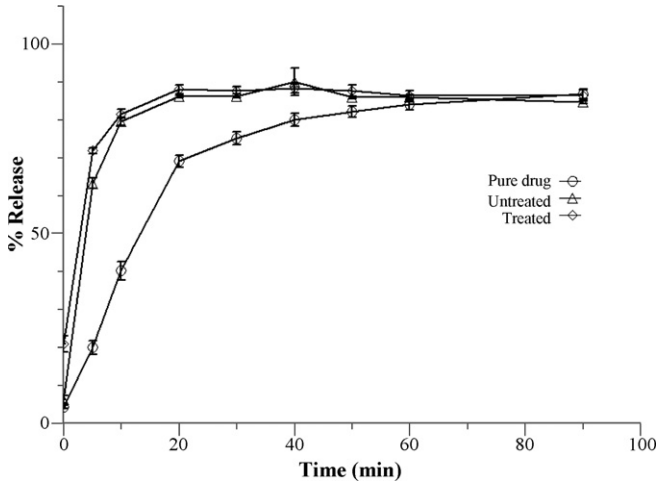

Fig. 8. The dissolution profile of PVP10k–CBZ (9:1) mixture.

similar trend was seen in the DSC studies for PVP10k:CBZ mixtures. For these samples as the amount of CBZ in the mixtures increased, the CBZ melting endotherms became more distinct and sharp. At the 9:1 ratio of PVP10k:CBZ, no CBZ endotherms were seen implying amorphous conversion in PVP10k matrix. At the 1:1 ratio CBZ melting endotherms were observed although attenuated in the treated samples implying some degree of amorphous change. However at the 1:9 ratio when the sample was dominated by CBZ, the sample essentially behaved like pure CBZ exhibiting sharp CBZ melting endotherms similar to pure CBZ in both untreated and treated samples.

Thus for the results obtained from X-ray, DSC and dissolution studies it was apparent that, only the lowest molecular weight PVP, PVP10k, exhibited the greatest conversion of crystalline CBZ to the amorphous form, at the above specified experimental conditions.

Spectroscopic studies (Kazarian et al., 2002) have shown that there is a Lewis acid–base type of interaction between CO_2 molecules and the lone pair of electrons on carbonyl groups of the polymers such as those present on the PVP chains. The

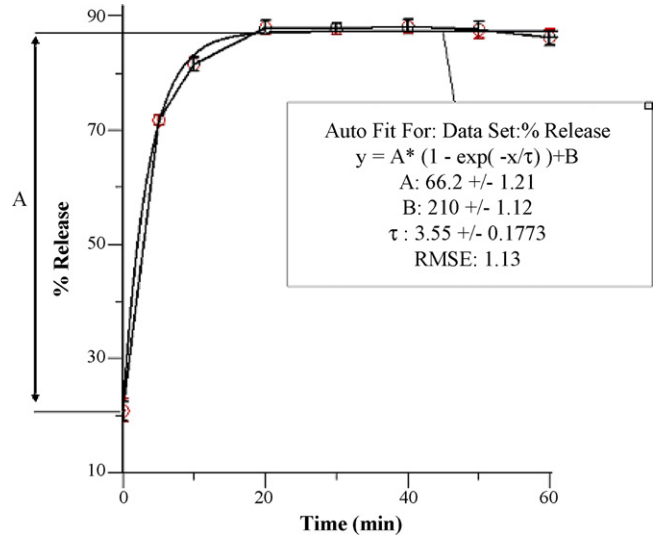

Fig. 9. Fitted dissolution curve of PVP10k:CBZ at 9:1 ratio.

carbonyl oxygen on the PVP chain donates its lone pair of electrons (Lewis base) to the carbon atom of the CO_2 (Lewis acid) which reduces interchain polymer interactions causing plasticization of the chains resulting in enhanced segmental and chain mobility and thus easing the path of diffusing solutes such as drug molecules to enter the polymer matrix. Kazarian (2002, 2004) in the work with the impregnation of ibuprofen molecules in PVP using supercritical carbon dioxide described the fact that when ibuprofen gets impregnated in the polymer there is a competitive interaction of ibuprofen and CO_2 molecules with the carbonyl groups of PVP. It was postulated that ibuprofen molecules interact through hydrogen bonding whereas the CO_2 molecules interact through Lewis acid–base interaction. The estimated strength of the Lewis acid–base interaction was in the order of 1 kcal mol^{-1} whereas for H-bond interaction, it was in the order of 2–4 kcal mol^{-1}. Applying this theory to our work, it can be proposed that when CBZ–PVP mixtures were subjected to n-$scCO_2$ treatment, the n-$scCO_2$ caused plasticization of PVP and partitioned the CBZ into the polymer matrix. There was a competitive interaction between the CO_2 molecules and $–NH_2$ groups of CBZ with the carbonyl groups of the PVP. Assuming that the hydrogen bonding interaction between $–NH_2$ group of CBZ with the carbonyl group of PVP was dominant in this case also, it would be expected that the CBZ molecules would be bound to the polymer sites, greatly reducing the crystallinity of CBZ. Yoshioka et al. (1995), Nair et al. (2001) and Sethia and Squillante, 2004 in their work with amorphous co-precipitates and solid dispersions have also attributed the inhibitory effect of PVP on the crystallization of a drug, to the interaction of the drug with PVP through hydrogen bonding.

However, though the Lewis acid–base type interaction and hydrogen bonding interaction theories explain the possible plasticization of PVP10k, easing the entry of CBZ in the PVP matrix and its ultimate reduction in the crystallinity, it should be noted that from the results obtained in this work, these theories did not seem to apply to the higher MW PVPs such as PVP29k, 55k and 130k, all of which share identical basic functional units similar to PVP10k. This may possibly be explained by considering the work carried out by Rindfleisch et al. (1996), which suggested that the entropy of mixing of CO_2 with a polymer is one of the primary determinants when assessing polymer solubility in $scCO_2$. Adequate mixing results in high diffusivity of CO_2 into the polymer, which is essential for enhanced segmental and chain mobility, which allows efficient impregnation of drug molecules. They theorized that in order to ensure adequate mixing, the CO_2 should first condense around the polymer. However, as the rotational flexibility of the chain segments decreases, which is likely to happen with increasing MW of the polymers, the number of possible polymer sites exposed to CO_2 decrease.

From this work we conclude that though the hydrogen-bonding interaction is the principal mechanism responsible for the reduction of CBZ crystallinity, the elementary interaction of CO_2 with the polymer dictates the degree of reduction of crystallinity. If the polymer is not sufficiently plasticized, the polymer chains will not allow efficient diffusion of drug molecules and the competitive interaction between the drug molecules and CO_2 with the carbonyl group of polymer would

result in little or no hydrogen bonding and thereby no reduction in the crystallinity.

It is likely that due to the experimental conditions utilized in our work only PVP10k plasticized to an appreciable extent. Thus, the higher MW PVPs and Na CMC failed to show any degree of conversion of CBZ to the amorphous form despite having the carbonyl group in the side chain. It is expected that as the pressure and temperature is increased in the system the higher MW polymers would show increase in rotational flexibility required to plasticize the polymer chains. However, to build a correlation between the plasticization of the polymers of different MW and different conditions of CO_2 is beyond the scope of this paper.

4. Conclusions

From the results obtained from the X-ray, DSC and dissolution studies for the conditions employed in this work we can draw following inferences.

The results from the X-ray, DSC and dissolution studies in this work demonstrated that when used as a solvent n-scCO_2 alone does not alter the crystallinity of pure CBZ. However, n-scCO_2 was effective in reducing the crystallinity of CBZ when combined with amorphous polymers. Of the two different types of polymers of varying molecular weights tested, CBZ combined with the lowest molecular weight PVP, PVP10k, showed a greater reduction in crystallinity as compared to the other high MW PVPs. CBZ in combination with different molecular weights of Na CMC demonstrated no measurable reduction in the crystallinity. This suggests that under the tested experimental conditions the rotational flexibility of the PVP10k allowed greater plasticization and thus increased diffusion of the drug into the polymer matrix as compared to the other higher MW polymers of both PVP and Na CMC. The ratio of polymer:drug is also a crucial determinant in increasing the dissolution of CBZ. Our studies indicated that a large particle size difference between the polymer and the drug particles could act as a source of variability leading to misinterpretation of the data. Hence, in order to minimize this variability it is desirable to achieve particle size as uniform as possible between the drug and the polymer.

Acknowledgements

The authors wish to thank URI Chemistry department for its DSC use and URI CELS department for the use of their high-resolution imaging system.

References

Behme, R., Brooke, D., 1990. Heat of fusion measurement of a low melting polymorph of carbamazepine that undergoes multiple-phase changes during differential scanning calorimetry analysis. J. Pharm. Sci. 80, 986–990.

Cansell, F., Aynmonier, C., Loppinet-Serani, A., 2003. Review on materials science and supercritical fluids. Curr. Opin. Solid State Mater. Sci. 7, 331–340.

Craig, D.Q.M., 2002. Review—the mechanisms of drug release from solid dispersions in water-soluble polymers. Int. J. Pharm. 231, 131–144.

Craig, D., Royall, P., Kett, V., Hopton, M., 1999. The relevance of the amorphous state to pharmaceutical dosage forms: glassy drugs and freeze dried systems. Int. J. Pharm. 179, 179–207.

Dobbs, J.M., Wong, J.M., Johnston, K.P., 1986. Non polar co-solvents for solubility enhancement in supercritical fluid carbon dioxide. J. Chem. Eng. Data 31, 303–308.

Doshi, D.H., Ravis, W.R., Betageri, G.V., 1997. Carbamazepine and polyethylene glycol solid dispersion preparation, in vitro dissolution, and characterization. Drug Dev. Ind. Pharm. 23, 1167–1176.

Han, J., Zhang, Y., Grant, G., Suryanarayanan, R., 2000. In situ dehydration of carbamazepine dihydrate: a novel technique to prepare amorphous anhydrous carbamazepine. Pharm. Dev. Tech. 5, 257–266.

Hancock, B.C., Zografi, G., 1997. Characteristics and significance of the amorphous state in pharmaceutical systems. J. Pharm. Sci. 86, 1–12.

Hancock, B.C., Shamblin, S., Zografi, G., 1995. Molecular mobility of amorphous pharmaceutical solids below their glass transition temperatures. Pharm. Res. 12, 799–806.

Kaneniwa, N., Ichikawa, J., Yamaguchi, T., Hayashi, K., Watari, N., Sumi, M., 1987. Dissolution behaviour of carbamazepine polymorphs. Yakugaku Zasshi 107, 808–813.

Kazarian, S.G., 2004. Supercritical Fluid Impregnation of Polymers for Drug Delivery. Supercritical Fluid Technology for Drug Product Development, vol. 138. Marcel and Dekker, p. 343.

Kazarian, S.G., Martirosyan, G.G., 2002. Spectroscopy of polymer/drug formulations processed with supercritical fluids: in situ ATR-IR and Raman study of impregnation of ibuprofen into PVP. Int. J. Pharm. 232, 81–90.

Kearney, A.S., Gabriel, D.L., Mehta, S.C., Radebaugh, G.W., 1994. Effect of polyvinylpyrrolidone on the crystallinity and dissolution rate of solid dispersions of the antiinflammatory CI-987. Int. J. Pharm. 104, 169–174.

Kobayashi, Y., Ito, S., Itai, S., Yamamoto, K., 2000. Physicochemical properties and bioavailability of carbamazepine polymorphs and dihydrate. Int. J. Pharm. 193, 137–146.

Krahn, F.U., Mielck, J., 1987. Relations between several polymorphic forms and the dihydrate of carbamazepine. Pharm. Acta Helv. 62, 247–254.

Lang, M., Kampf, J.W., Matzger, A.J., 2002. Form IV of carbamazepine. J. Pharm. Sci. 91, 1186–1190.

Lőbenberg, R., Amidon, G.L., 2000. Modern bioavailability, bioequivalence and biopharmaceutics, classification system. New scientific approaches to international regulatory standards. Eur. J. Pharm. Biopharm. 50, 3–12.

Moneghini, M., Kikic, I., Voinovich, D., Perissutti, B., Filipović-Grčić, 2001. Processing of carbamazepine-PEG 4000 solid dispersions with supercritical carbondioxide: preparation, characterization, and in vitro dissolution. Int. J. Pharm. 222, 129–138.

Mukhopadhyay, M., 2004. Phase equilibrium in solid–liquid-supercritical fluid systems supercritical fluid technology for drug product development. 32, 27.

Nair, R., Nyamweya, N., Gönen, Martínez-Miranda, Hoag, S.W., 2001. Influence of various drugs on the glass transition temperature of poly(vinylpyrrolidone): a thermodynamic and spectroscopic investigation. Int. J. Pharm. 225, 83–96.

Nair, R., Gonen, S., Hoag, S.W., 2002. Influence of polyethylene glycol and povidone on the polymorphic transformation and solubility of carbamazepine. Int. J. Pharm. 240, 11–22.

Rindfleisch, F., DiNoia, T.P., McHugh, M.A., 1996. Solubility of polymers and copolymers in supercritical CO_2. J. Phys. Chem. 100, 15581–15587.

Sethia, S., Squillante, E., 2004. Solid dispersion of carbamazepine in PVP K-30 by conventional solvent evaporation and supercritical methods. Int. J. Pharm. 272, 1–10.

Simonelli, A.P., Mehta, S.C., Higuchi, W.I., 1976. Dissolution rates of high energy sulfathiazole-povidone coprecipitates. II. Characterization of form of drug controlling its dissolution rate via solubility studies. 65, 355–361.

Taylor, J.R., 1982. An Introduction to Error Analysis: The Study of Uncertainties in Physical Measurements. Oxford University Press, Chapter 3, p. 57.

Thumsi, S.G., 2004. Investigating the effect of supercritical fluid in characterization of nifedipine and possible improvement of dissolution. Master of Science Thesis, University of Rhode Island, USA, p. 123.

Warren, B.E., 1969. X-ray Diffraction. Addison Wesley publication, pp. 331–332.

Yoshioka, M., Hancock, B.C., Zografi, G., 1995. Inhibition of indomethacin crystallization in poly(vinylpyrrolidone) coprecipitates. J. Pharm. Sci. 84, 983–986.